ESRF	**Experiment title:** GIDAFS and EXAFS Study of InAs/InP buried Quantum Sticks	**Experiment number:** HS 1024, 0202-607 , 3002-636
Beamline: BM32, BM02, BM30b	**Date of experiment:** from: 05/03/03 to:11/03/03, 17/0703 22/07/03 18/06/03 21/06/3	**Date of report:** 01/09/04
Shifts: 18, 15,15	**Local contact(s):** H. Renevier, J.S. Micha, X. Biquard	*Received at ESRF:*

Names and affiliations of applicants (* indicates experimentalists):

A. Letoublon[1,2], V. Favre-Nicolin[1,2], H. Renevier[1,2], M.G. Proietti[3]

[1]Commissariat à l'Energie Atomique, Département de Recherche Fondamentale sur la Matière Condensée, SP2M/NRS, 17 rue des martyrs, 38054 Grenoble Cedex 9, France.
[2]Université Joseph Fourier, BP 53, F-38041, Grenoble Cedex 9, France.
[3]Departamento de Física de la Materia Condensada, Instituto de Ciencia de Materiales de Aragón, CSIC-Universidad de Zaragoza - c. Pedro Cerbuna 12, 50009 Zaragoza, Spain.
Hubert.Renevier@cea.fr

NB: *This experimental report exceeds the foreseen three pages length since it referes to three experiments the results of which are complementary and compared in the report text (HS 1024, 0202 607 and 3002-636)*

Introduction

We report on an x-ray study of InAs stick-like islands (QSs) embedded in InP with a 10 nm thick cap layer. These samples are obtained by optimisation of the MBE growth parameters to minimize the As/P exchange and reduce the height dispersion of the InAs islands [1]. Strain of buried nanostructures is related to composition but it also depends on size, morphology, and cap layer thickness. Tuning the x-ray energy near an absorption edge of atoms that belong to the nanostructures is a way to modify their scattering power and to enhance the chemical sensitivity of diffraction and eventually obtaining direct information on compostion [2, 3, 4]. We report on a general method that takes advantage of the full capability of anomalous diffraction and can be applied to the very interesting and challenging case of small size embedded nanostructures [5].

Results and discussion

Grazing incidence Anomalous diffraction at the As K-edge (11.867 keV) was performed at the French Collaborative Research Group beamlines BM32 and BM2. Figure 1 shows the diffraction intensity map in the vicinity of the (442) InP substrate reflection, recorded at 11.840 keV and at a grazing incidence angle near to the critical angle (0.2°). The spreading of scattering along the [110] direction is due to both short range correlation and lattice strain, whereas, in the [001] direction, it is due to the sharp strain evolution at interface. We performed *l*-scans (h=k=3.98) across the satellite S1, at several energies close to the As *K*-edge. Figure 2a shows the experimental modulus of F_{As},

i.e. the As atoms partial structure factor, and F_T, the structure factor calculated with all atoms but excluding the As anomalous terms. As deduced from the Full Width at Half Maximum (FWHM) of F_{As}, the QSs height average value is about 2.54nm.

Finite Difference Method simulations were performed to map the strain produced by InAs QSs embedded in InP and compare its Fourier Transform to experimental diffraction intensity maps. Figure 2a shows the best calculated curves of F_{As} and F_T, obtained by optimizing the height and width of the wires, as well as As/P intermixing at the InAs/InP interface. The FDM simulation reproduces well the relative positions of F_{As} and F_T, with a strain of about 6.1% in the inner part of the wire. The experimental curves F_{As} and F_T are compatible with a weak As/P intermixing at the InP interface, that would spread over one ML.

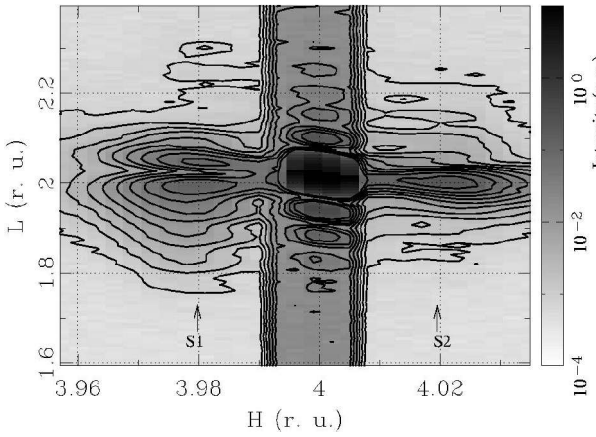

Fig. 1: Experimental diffraction map around the weak InP (442) reflection recorded at 11.840 keV in grazing incidence geometry ; S1 and S2 are correlation satellites due to the stick short range periodicity along the [110] direction.

To determine precisely the QSs composition and the local strain accommodation inside the QSs, we measured fix-Q anomalous diffraction spectrum in grazing incidence (Grazing Incidence Diffraction Anomalous Fine Structure, GIDAFS), at the As K-edge, at the maximum of F_{As} (h=k=3.98 and l=1.9). Figure 2b shows the experimental DAFS spectrum and the calculated curve obtained with the As anomalous scattering factors of bulk InAs. The best fit curve, shown on figure 2b corresponds to an As concentration x=1.03 ($A_{1-x}P_x$ inside the QSs), i.e. the QSs composition is pure InAs.

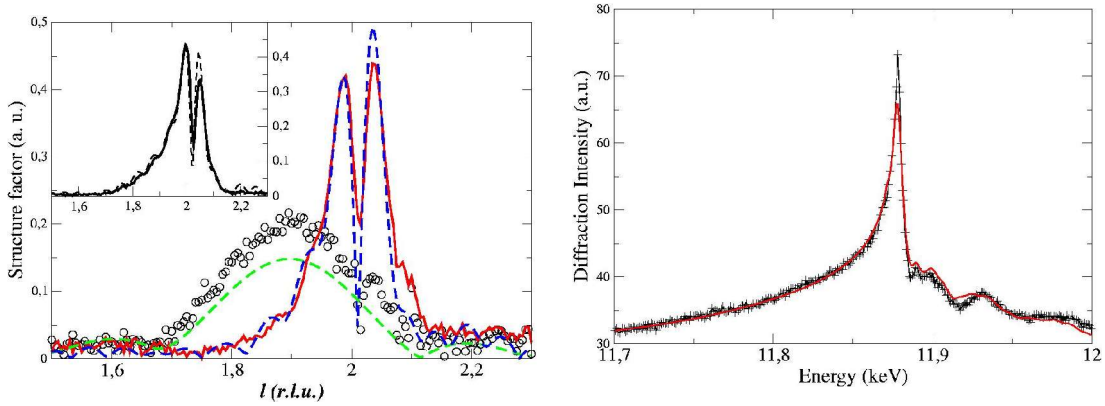

Fig. 2: (a) Experimental F_T (solid line) and F_{As} (ooo) modulus as a function of the reciprocal lattice unit l at h=k=3.98 (across the satellite S1). F_{As} is the structure factor of all anomalous atoms, i.e. As atoms only. Also shown are best simulation curves (dashed line) obtained with a Finite Difference Model made of pure InAs QSs with a truncated triangle side profile. Inset shows the experimental (solid line) and simulated (dashed line) square root of the diffraction intensity at 11.867keV ; at this energy, anomalous diffraction is maximized. (b) Fixed-Q anomalous diffraction spectra (-) recorded, at the As K-edge, at the maximum of the F_{As} profile (l=1.9) and the best fit curve obtained with pure InAs structure (solid line).

Further information about composition and strain can be achieved by quantitative analysis of the DAFS oscillations, showing up in the extended region after the absorption edge. We

show in figure 3 this fine structure extracted from the smooth atomic background. The signal-to-noise ratio must be improved to perform an accurate quantitative analysis and the energy (k) range extended. Nevertheless, we show here a preliminary experiment and analysis with the aim of illustrating the technique capabilities. The analysis can be performed according to the standard criteria and available codes for Extented X-ray Absorption Fine Structure, provided that crystallographic phase and amplitude correction factors are taken into account [6]. The DAFS oscillations has been then analysed by fitting the theoretical signal to the experiment by means of the Ifeffit code [7]. Theoretical phase and amplitudes have been calculated for a bulk InAs cluster by the FEFF8 code [8], with the incident photon polarization parallel to the [001] direction (i.e. perpendicular to the surface).

The parameters that were allowed to vary and the fit results are reported in Table I and figure 3. The latter shows the comparison of the DAFS spectrum with the best fit theoretical curve. We iterated the Nearest Neighbour distance As-In_I distance (NN), the Next Nearest Neighbour (NNN) distance As-As_{II} and the three legs multiple scattering (MS) path As_{abs}-In_I-As_{II} and As_{abs}-In_I-P_{II}. The values found are in agreement with mismatch strained InAs. The relevant result from table I is that, to improve the fit quality NNN and triangular MS paths involving P atoms are to be included. The presence of P is simulated by adding scattering paths in which the As scatterer is substituted by P, with a population factor x ((1-x) for As). The NNN As-P_{II} distance is found to be equal to 4.18Å. It is shorter than what expected for an InAsP alloys [9] suggesting that the P atoms are mostly located at the InAs/InP interface. This confirms the anomalous diffraction results showing that the QSs region contributing to diffraction is essentially made of InAs.

EXAFS measurements have also been performed, on the same sample, at the As K-edge with the polarization vector perpendicular and parallel to the growth plane. The measurements were performed at the French CRG FAME beamline (exp. ref. n. 30-02-636). The perpendicular and parallel EXAFS spectra were fitted simultaneously (multifit) by means of Ifeffit package implemented by the Artemis interface program [7]. Theoretical phases and amplitudes were calculated, taking into account polarization, by Feff8 code [8]. The interatomic distances iterated in the fit procedure corresponded to the first (As_{abs}-In_I), second (As_{abs}-As_{II} and As_{abs}-P_{II}) and third (As-In_{III}) coordination shells. The Debye-Waller factors were also iterated as well as the P concentration. Due to light polarization and monocrystalline nature of the samples, the A_{sabs}-As_{II} , As_{abs}-P_{II} and As-In_{III} scattering paths are no longer equivalent and they are splitted out in the in-plane and out-of-plane contributions. In-plane and out-of-plane As_{abs}-P_{II} scattering paths have its own P population, x and y respectively, as a fit parameter. The same kind of triangular multiple scattering paths, As_{abs}-In_I-As_{II} and As_{abs}-In_I-P_{II} , were included as for DAFS, but they were determined by the NN and NNN distances found by the multifit. The multifit results are shown in Table II and figure 5. We can observe the following findings:

i) The As_{abs}-In_I distance is slightly contracted as for the DAFS spectrum, in agreement with the presence of mismatch strain.
ii) For the As_{abs}-As_{II} NNN distance we find two values: 4.15Å (in-plane) and 4.24Å (out-of-plane). The first one is equal to the InP distance in bulk InP, i.e. is the value expected for pseudomorphic InAs on inP. The second one is shorter than what expected for pseudomorphic InAs (4.29Å) and what found for DAFS (4.30Å).
iii) The in plane and out-of-plane As_{abs}-P_{II} distances are found to be 4.18 Å and 4.17Å respectively, i.e. practically the same.
iv) The P concentration is found to be quite high, higher than for DAFS, showing a difference between in-plane and out-of plane P coordination, the latter being the highest.
v) The As-In_{III} third coordination shell distance shows two values: 4.88Å and 4.93Å. The first one is close to the value expected for pseudomorphic InAs, nevertheless the further distance found is also contracted with respect to the bulk InAs value (5.023Å), i.e. the expected pseudomorphic elongated distance (5.13Å) is not observed.

Comparing with the DAFS results we find an apparent discrepancy: a higher P concentration and a shorter As-P out of plane distance. The difference between the EXAFS and DAFS data is well illustrated in fig.3 where the DAFS best fit (continuous curve) is compared with the EDAFS calculated according to reference [6] from the EXAFS best fit χ, and the cristallographic phase $\Delta\phi$. The two curves are clearly different, out of the DAFS measurement noise.

To explain the EXAFS results, i.e. the contracted As_{abs}-As_{II} NNN and As-In_{III} out-of-plane distances, and the higher P concentration, we should admit the presence of a certain amount of As/P intermixing. This seems to be at odd with the DAFS analysis showing pure InAs wires. On the other hand, the discrepancy is only apparent due to the different selectivities of the two techniques. EXAFS is *chemically* selective, DAFS instead, is *chemically and spatially* selective. Can we state that in this case we are probing, by the two techniques, different regions in the sample? Fig. 4 shows the relative contribution of the As atoms to the total F_{As} structure factor calculated at the maximum of F_{As} (Q=3.985, 3.985, 1.9). It can be seen that the central part (lateral direction) is the dominant contribution. DAFS is then more sensitive to the As atoms belonging to the inner part of the wires than to those belonging to the wires lateral tails. Moreover a certain amount of As atoms, probed by EXAFS, could be dispersed over one or two monolayers of the capping layers. Considering the small equivalent QWrs thickness (2.2MLs) this could be enough to increase appreciably the P concentration and to introduce shorter As-As distances typical of diluted InAsP alloys.

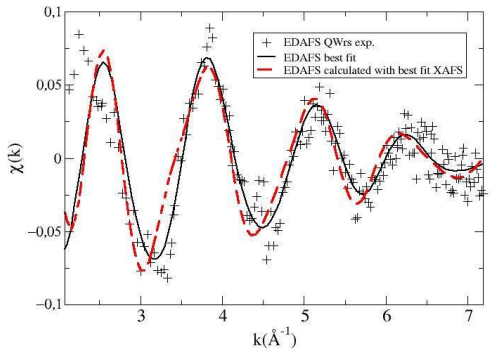

Fig. 3: Extended DAFS spectrum of embedded InAs QSs (+++) compared with best fit theoretical curve (continuous line) and the calculated DAFS spectrum obtained from best fit of absorption spectrum.

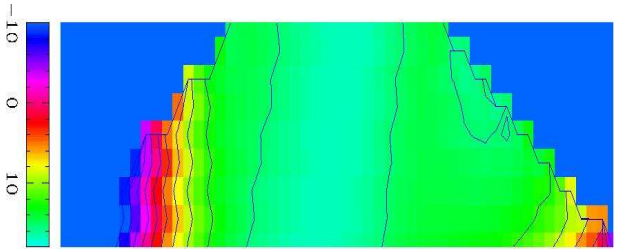

Fig. 4: Cross section of an InAs QWr embedded in InP calculated with the Finite Difference Method. The color scale shows the relative contribution of the As atoms to the As structure factor F_{As} (Q=3.985, 3.985, 1.9). It can be seen that the central part of the wire (lateral direction) is the dominant contribution.

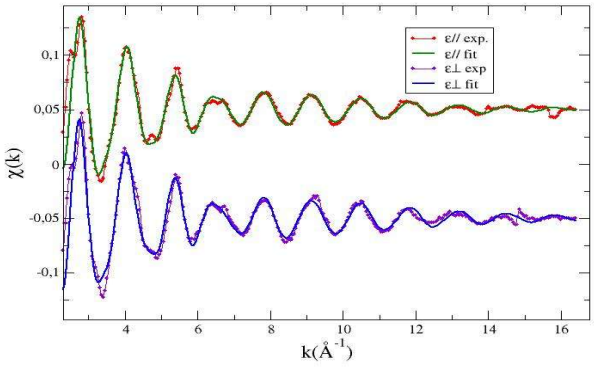

Fig. 5: Multifit results (solid continuous curves) compared with the experimental EXAFS signals (dotted curves) for $e_{//}$ (upper curves) and e (lower curves).

Path	Distance (Ă)	**σ ² (Ă²)**
As_{abs}-In_I	2.58 ± 0.001	0.007 ± 0.004
$(As_{abs}$-$As_{II})_{\perp}$	4.30 ± 0.08	0.017 ± 0.009
$(As_{abs}$-$P_{II})_{\perp}$	4.18 ± 0.04	0.017 ± 0.009
As_{abs}-In_I-As_{II}	4.73 ± 0.02	0.017 ± 0.009
As_{abs}-In_I-P_{II}	4.64 ± 0.02	0.017 ± 0.009
S_D	***Phase (rad)***	***x***
0.560±0.09	0.5	0.48 ± 0.14

Table I : EDAFS best fit values for interatomic distances, Debye-Waller factors and P concentration (x) obtained by IFEFFIT mimimization [6] using theoretical fitting standards provided by FEFF8 code [8]. The amplitude and phase correction factors have been obtained by cristallographic analysis of the DAFS lineshape [7, 2].

TableII

Path	Distance (Ă)	**σ ² (Ă²)**
As_{abs}-In_I	2.59± 0.002	0.003 ± 0.004
$(As_{abs}$-$As_{II})_{//}$	4.15 ± 0.06	0.010 ± 0.004
$(As_{abs}$-$As_{II})_{\perp}$	4.24 ± 0.04	"
$(As_{abs}$-$P_{II})_{//}$	4.18 ± 0.06	"
$(As_{abs}$-$P_{II})_{\perp}$	4.17 ± 0.03	"
As_{abs}-In_I-As_{II}	4.70	0.0009 ± 0.004
As_{abs}-In_I-P_{II}	4.65	"
$(As_{abs}$-$In_{III}))_{//}$	4.88± 0.03	0.028 ± 0.006
$(As_{abs}$-$In_{III})_{\perp}$	4.93± 0.06	"
S_0	***x***	***y***
0.78±0.03	0.38± 0.15	0.57 ± 0.11

TableII : EXAFS best multifit values for interatomic distances, Debye-Waller factors and P concentration (x) obtained by IFEFFIT mimimization [6] using theoretical fitting standards provided by FEFF8 code [8] and Artemis interface. // and stand for in-plane and out-of-plane scatterimng paths.

References

[1] M. Gendry, C. Monat, J. Brault, P. Regreny, G. Hollinger, B. Salem, G. Guillot, T. Benyattou, T. C. Bru-Chevallier, G. Bremond, O. Marty. J. Appl. Phys 95, 4761 (2004).

[2] J.L. Hodeau, V. Favre-Nicolin, S. Bos, H. Renevier, E. Lorenzo, J.F. Bérar, Chem. Rev., 101, (2001), 1843.

[3] S. Grenier, M.G. Proietti, H. Renevier, L.González, J.M. García and J. García, Europhys. Lett., 57, 449 (2002).

[4] T. Schülli, J. Stangl, Z. Zhong, R. Lechner, M. Sztucki, T. Metzger, G. Bauer, Phys. Rev. Lett. 90, 066105 (2003).

[5] A. Létoublon, V. Favre Nicolin, H. Renevier, M.G. Proietti, M. Gendry, C. Monat, O. Marty, C. Priester, Phys. Rev. Lett. 92, 186101 (2004).

[6] M.G. Proietti, H. Renevier, J.L. Hodeau, J. García, J.F. Bérar, P. Wolfers, Phys. Rev. B 59, 5479 (1999).

[7] M. Newville, J. Synchrotron Rad. **8**, 322 (2001).

[8] A.L. Ankudinov, B. Ravel, J.J. Rehr, S.D. Conradson, Phys. Rev. B 58, 7565 (1998).

[9] S. Pascarelli, F. Boscherini, C. Lamberti, S. Mobilio, Phys. Rev. B 56, 1936 (1997).